

Cite this: DOI: 10.1039/c0xx00000x

www.rsc.org/xxxxxx

## Supplementary Information

# Tuning electronic transport in cobalt-filled carbon nanotubes using magnetic fields

Francesco Rossella,<sup>\*a,‡</sup> Caterina Soldano,<sup>b</sup> Pasquale Onorato<sup>a</sup> and Vittorio Bellani<sup>a</sup>

Received (in XXX, XXX) Xth XXXXXXXXX 20XX, Accepted Xth XXXXXXXXX 20XX

DOI: 10.1039/b000000x

## Methods

Alumina template (AAO) grown carbon nanotubes investigated in the present work have a diameter of approximately 100 nm and an average length between 10 and 20  $\mu\text{m}$ . The details of the metal filling procedure of AAO-CNTs with cobalt clusters are reported elsewhere.<sup>12</sup> The Raman spectra were measured with a micro-Raman set-up (Horiba Jobin-Yvon Labram HR) with  $\sim 1 \text{ cm}^{-1}$  spectral resolution, using a 100X objective (laser spot  $\sim 1 \mu\text{m}$ ) and an excitation wavelength of 632.81 nm. The spatial resolution is smaller than 500 nm, the acquisition time was of the order of few minutes, and the incident power was  $\sim 5 \text{ mW}$ . The tubes were dispersed from a IPO-based solution onto a Si/SiO<sub>2</sub> substrate, and standard electron-beam lithography was used to fabricate the electrical contacts (5/60 nm of Ti/Au) on individual tubes. Standard AC lock-in techniques have been used for transport experiments performed at zero-magnetic fields, while high impedance DC electrometer have been employed during the experiments in low- and high-magnetic fields. A pulsed magnetic field was applied in the direction perpendicular to the tube axis. The magnetic field pulse, with a peak value of  $\sim 50 \text{ T}$  and duration of  $\sim 350 \text{ ms}$ , was generated energizing a copper coil immersed in liquid nitrogen with energy of 14 MJ (stored in a capacitor bank).

## Device processing

Electron beam lithography has been used to fabricate electrodes and side gates on individual Co-filled CNTs deposited on SiO<sub>2</sub>/Si substrates, with typical tube dimensions of 50-100 nm diameter and 10-20  $\mu\text{m}$  length. The devices have typically 6 comb-like electrodes, a back gate and two side gates allowing the application of a voltage.

## Variable Range Hopping as Possible Mechanism for $G(T)$

The two-dimensional variable range hopping (VRH) model has been previously used to describe the electronic conduction in highly disordered systems such as template-grown nanotubes [1]. In this model, the electron wave-function becomes strongly localized due to the presence of disorder, with a vanishing conductance in the limit of zero temperature. At finite temperature, the conduction occurs through a thermally activated hopping between localized states, in which an electron lying in an occupied state below the Fermi energy receives energy from a phonon, which enables the hopping of the electron to a nearby

state above the Fermi level. At low temperatures, the most frequent hopping process is not necessarily to the nearest neighbor. In this model, the conductance varies as  $G(T) \approx \exp[-(T_0/T)^{1/(1+d)}]$  where  $d$  is the dimensionality of the system and  $T_0$  a characteristic temperature. This temperature  $T_0$  is related to the 2D density of states,  $N_{2D}$  at the Fermi energy  $N_{2D}(E_F)$ , the hopping length ( $L_{hop}$ ) and the localization length ( $L_{loc}$ ) according to  $T_0 = 13.8/[N_{2D}(E_F)L_{loc}^2 K_B]$  and  $L_{hop}(T) = (L_{loc}/3)(T_0/T)^{1/3}$  [2].

We applied this model to our data, estimating  $N_{2D}(E_F)$  from the bulk density of state ( $\approx 10^{18}/\text{eVcm}$ , typical of amorphous carbon [3]), multiplied by the tube thickness ( $d_0 = 10 \text{ nm}$ ) [4]. Dashed line in Fig. S-1 represents the fit according to the VRH mechanism of the temperature dependence of the zero-field conductance ( $G$ ) of our devices, assuming  $d = 2$ . In principle, at low temperature the deviation between the experimental data and the theoretical curve could be due to a dependence of the scattering rates on the energy of the injected electrons. The best fit gives  $T_0 = 0.9 \text{ K}$  leading to  $L_{loc} \sim 4.2 \mu\text{m}$ , and hence,  $L_{hop} \sim 200 \text{ nm}$  and  $\sim 1.1 \mu\text{m}$ , at room temperature and 2 K respectively. These values appear not realistic, in particular the value of  $T_0$ , which represents the temperature below which the VRH model is valid, and clearly cannot be lower than the temperature range of the experimental data if we intend to apply this model.

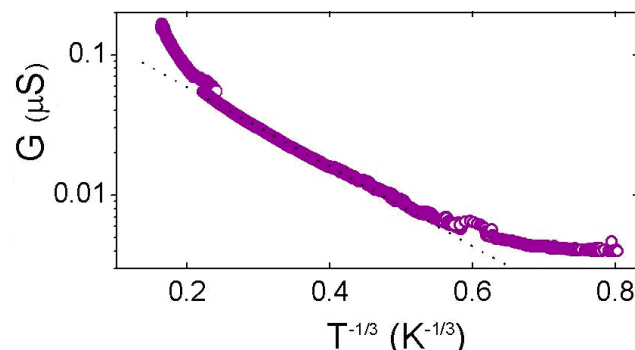


**Figure S-1** Temperature dependence of the zero-field linear conductance from 230 K down to  $\sim 2 \text{ K}$ ; the conductance is plotted as function of  $T^{-1/3}$ . The dashed line represents the fit using the VRH model.

## Conductance and Weak Localization

The corrections  $\delta G(B) = G(B) - G(B=0)$  to the weak localization (WL) conductance due to a weak magnetic field can

be calculated for one-dimensional systems using first order perturbation theory by Altshuler and Aronov [5]:

$$G(B) = -g_S g_v (e^2/h)(1/L)[(D\tau_\phi)^{-1} + (D\tau_B)^{-1}]^{-1/2} \quad (1),$$

where  $g_S$  and  $g_v$  are the spin and valley degeneracies,  $L$  length of the channel,  $\tau_\phi$  is the phase coherence time,  $D = v_F^2 \tau/2$  is the diffusion constant,  $\tau = m\mu_e/e$  is the scattering time,  $\mu$  is the electron mobility,  $\tau_B = 3l_B^4/W^2 D$  is the magnetic relaxation time,  $l_B = (h/eB)^{1/2}$  is the magnetic length and  $W$  is the width of the channel. If we introduce a pre-factor  $g=g_S g_v e^2/h$ , we obtain:

$$\delta G = -(g/L)[(D\tau_\phi)^{-1} + (D\tau_B)^{-1}]^{-1/2} \quad (2).$$

Eliminating  $D$  from Eq. (2) by rewriting  $D\tau_\phi$  as  $l_\phi^2$ , and  $D\tau_B$  as  $3l_B^4/W^2$ , we get:

$$\delta G = -(g/L)(1/l_\phi^2 + 1/3l_B^2/W^2)^{-1/2} \quad (3).$$

Introducing the definition of  $l_B$ , we have:

$$\delta G = -(gl_\phi/L)[1 + e^2B^2/(3h^2/l_\phi^2W^2)]^{-1/2} \quad (4).$$

If we introduce the parameter  $B_\phi^2 = 3h^2/e^2l_\phi^2W^2$ , Eq.(4) becomes:

$$\delta G = -(gl_\phi/L)(1 + B^2/B_\phi^2)^{-1/2} \quad (5).$$

Rewriting Eq. (5) in terms of the resistance correction:  $\delta R = R(B) - R(0) = 1/G(B) - 1/G(0) = 1/[\delta G + G(0)] - 1/G(0)$ . Let's call  $\delta G = x$ , so that  $\delta R$  results a function of  $x$  in the form  $f(x) = 1/[G(0) + x]$ .

In the limit of  $x \ll G(0)$ , we can expand  $f(x)$  in the Taylor series at the first order, obtaining:  $f(x) \sim f(x=0) + x f'(x=0) \cdot x = 1/G(0) - x/[G(0)+x]^2 \cdot x$ , where we can neglect  $x^2$ , resulting in  $f(x) \sim 1/G(0) - x/G(0)^2$ .

If we substitute this expression in  $\delta R$ , we have:  $\delta R \sim 1/G(0) - \delta G/G(0)^2 - 1/G(0) = -\delta G/G(0)^2 = (gl_\phi/LG(0)^2)(1 + B^2/B_\phi^2)^{-1/2}$ , which provides the corrections to the WL resistance due to the magnetic field  $B$ .

A negative magneto-resistance behavior can also be accounted for within the picture of a two-dimensional WL regime [S-7], with the following expression valid for  $l_\phi \gg W$ :

$$[R(B) - R(0)]/R(0) = -R(0)e^2/(2\pi^2\hbar)[\Psi(1/2 + \hbar/4e l_\phi^2 B) - \ln(\hbar/4e l_\phi^2 B)] \quad (6),$$

where  $\Psi$  is the Digamma function. Manipulating Eq. (6) similarly to the case of the 1D system, we get:  $\delta G \approx g_0[\Psi(1/2 + B_H/B) - \ln(B_H/B)]$ , where we introduce the fitting parameter  $B_H$ . This expression of  $\delta G$  allows fitting the experimental data with  $B_H \approx 0.02$  T and  $l_\phi = (1/2)(\hbar/eB_H)^{1/2} \approx 26/2(0.02)^{1/2}$  nm  $\approx 90$  nm.

## Bias Dependence of the Conductance

Let us assume a linear dependence of the conductance on the applied bias voltages (*i.e.*  $G(V) \approx \gamma V$ ), so that we can write the following expressions for the high- and zero-field conductance:  $G_\infty(V) = G_\infty(0) + \gamma V$  and  $G_0(V) = G_0(0) + \gamma V$ , where  $G_\infty(0)$  and  $G_0(0)$  are the zero-bias quantum conductances at high- and zero-field, respectively.

If we set  $\delta G = G_\infty(0) - G_0(0)$ , we can rewrite the previous expressions as:  $G_\infty(V) = G_0(0) + \delta G + \gamma V$  and  $G_0(V) = G_0(0) + \gamma V$ . Then we obtain the following expression for:  $G_\infty(V)/G_0(V) = (G_0(0) + \gamma V)/(G_0(0) + \gamma V) + \delta G/(G_0(0) + \gamma V) = 1 + \delta G/(G_0(0) + \gamma V)$ .

+  $\gamma V$ .

Finally, introducing the parameters  $\alpha = \delta G/G_0(0)$  and  $\beta = \gamma/G_0(0)$ , we get:  $G_\infty(V)/G_0(V) = 1 + \alpha/(1 + \beta V)$ .

## References

1. W. Y. Jang, N. N. Kulkarni, C. K. Shih and Z. Yao, *Appl. Phys. Lett.* 2004, **84**, 1177.
2. B. I. Shklovskii, and A. L. Efros, *Electronic properties of doped semiconductors*, Springer, Berlin, 1984.
3. J. J. Hauser, *Journal of Non-Crystalline Solids* 1977, **23**, 21. Th. Frauenheim, U. Stephan, K. Bewilogua, F. Jungnickel, P. Blaudeck and E. Fromm, *Thin Solid Films* 1989, **182**, 63.
4. C. Soldano, S. Kar, S. Talapatra, S. Nayak and P. M. Ajayan, *Nano Letters* 2008, **8**, 4498.
5. C. Mora, R. Egger and A. Altland *Phys. Rev. B* 2007, **75**, 035310. B. L. Altshuler, A. G. Aronov, *Electron-Electron Interactions in Disordered Systems*, Ed. by A. L. Efros and M., Pollak, North-Holland, Amsterdam, 1985.
6. S. N. Song, X. K. Wang, R. P. H. Chang and J. B. Ketterson, *Phys. Rev. Lett.* 1994, **72**, 697.